

Ionization constants of aqueous amino acids at temperatures up to 250°C using hydrothermal pH indicators and UV-visible spectroscopy: Glycine, α -alanine, and proline

RODNEY G. F. CLARKE,¹ CHRISTOPHER M. COLLINS,¹ JENENE C. ROBERTS,¹ LILIANA N. TREVANI,^{1,2} RICHARD J. BARTHOLOMEW,^{1,2,3} and PETER R. TREMAINE,^{1,2,*}

¹Department of Chemistry, Memorial University of Newfoundland, St. John's, NL, Canada A1B 3X7

²Guelph-Waterloo Centre for Graduate Work in Chemistry, University of Guelph, Guelph, ON, Canada N1G 2W1

³University of Ontario Institute of Technology, Oshawa, ON, Canada L1H 7L7

(Received January 20, 2004; accepted in revised form November 2, 2004)

Abstract—Ionization constants for several simple amino acids have been measured for the first time under hydrothermal conditions, using visible spectroscopy with a high-temperature, high-pressure flow cell and thermally stable colorimetric pH indicators. This method minimizes amino acid decomposition at high temperatures because the data can be collected rapidly with short equilibration times. The first ionization constant for proline and α -alanine, $K_{a,COOH}$, and the first and second ionization constants for glycine, $K_{a,COOH}$ and $K_{a,NH4+}$, have been determined at temperatures as high as 250°C. Values for the standard partial molar heat capacity of ionization, $\Delta_r C_p^{\circ,COOH}$ and $\Delta_r C_p^{\circ,NH4+}$, have been determined from the temperature dependence of $\ln(K_{a,COOH})$ and $\ln(K_{a,NH4+})$. The methodology has been validated by measuring the ionization constant of acetic acid up to 250°C, with results that agree with literature values obtained by potentiometric measurements to within the combined experimental uncertainty.

We dedicate this paper to the memory of Dr. Donald Irish (1932–2002) of the University of Waterloo—friend and former supervisor of two of the authors (R.J.B. and P.R.T.). Copyright © 2005 Elsevier Ltd

1. INTRODUCTION

The properties of amino acids in hydrothermal solutions are of interest to biochemists and geochemists studying metabolic processes of thermophilic organisms and possible mechanisms for the origin of life at deep ocean vents. Thermophilic bacteria and archaea have been found to exist at temperatures up to 121°C. Much more extreme conditions are encountered at deep ocean hydrothermal vents, where reduced aqueous solutions from deep under the sea floor are ejected into cold, oxidizing ocean water at temperatures and pressures that may reach near-critical and even super-critical conditions. The resulting solutions are rich in organic molecules, including amino acids, and it has been postulated that similar hydrothermal vents on primitive Earth may have been sites for the origin of life (Baross and Demming, 1983; Trent et al., 1984; Yanagawa and Kojima, 1985; Miller and Bada, 1988; Shock, 1990, 1992; Bada et al., 1995; Crabtree, 1997). This hypothesis is not without controversy, and it is an active topic of study through both field and laboratory investigations.

To investigate mechanisms for the abiogenic synthesis of polypeptide molecules, reliable experimental thermodynamic data must be obtained, under hydrothermal conditions, for the speciation of amino acids, the formation of peptide bonds, and the complexation of amino acids with metal ions, both in the aqueous phase and at mineral interfaces.

The challenges in measuring thermodynamic constants for the amino acids under these conditions are formidable, and only a few quantitative studies at elevated temperatures have been reported. Heat-of-mixing flow calorimetry has been used to determine ionization constants and enthalpies of reaction for

the protonation of the amino and carboxylate groups of several amino acids at temperatures of up to 125°C (Izatt et al., 1992; Gillespie et al., 1995; Wang et al., 1996). Vibrating-tube densimeters and a Picker-type flow microcalorimeter have recently been used to determine experimental values for the standard partial molar volumes and heat capacities of glycine, α -alanine, β -alanine, proline, and the dipeptide glycyl-glycine, at temperatures as high as 275°C (Hakin et al., 1995, 1998; Clarke and Tremaine, 1999; Clarke et al., 2000). We are aware of no other experimental studies on the thermodynamic properties of aqueous amino acids or peptides above 100°C.

Amino acids exist in aqueous solutions at room temperature as zwitterions, $HA^{\pm}(aq)$. The carboxylate and ammonium ionic groups can ionize to yield protonated and deprotonated forms of the amino acid, according to the following equilibria:



The equilibrium concentration of the nonzwitterionic form $HA^{\circ}(aq)$ is negligible at room temperature (Cohn and Edsall, 1943).

The most widely reported methods for determining acid-base dissociation constants under hydrothermal conditions are potentiometric titrimetry and conductivity (Mesmer et al., 1970, 1997; Ho et al., 2000). Conductivity measurements of amino acid ionization constants are impractical because, according to reactions 1 and 2, an excess of acid or base is required to drive the ionization. The use of pH titrations in the usual stirred hydrogen concentration cells (Mesmer et al., 1970) to study amino acids is limited to relatively low temperatures because amino acids have limited stability under hydrothermal conditions (Povoledo and Vallentyne, 1964; Vallentyne, 1964, 1968; Bada and Miller, 1970). The length of time required to achieve

* Author to whom correspondence should be addressed (tremaine@uoguelph.ca).

thermal equilibrium and to conduct the titration causes the amino acids to decompose. Although flow cells exist for potentiometric titrimetry (Sweeton et al., 1973; Lvov et al., 1999), they are complex to operate and have been used in only a few studies (e.g., Patterson et al., 1982).

Recent work at the University of Texas (Austin) has identified five thermally stable colorimetric pH indicators, which have been used with success in UV-visible spectrophotometric flow cells to determine ionization constants of simple acids and bases at temperatures as high as 400°C (Ryan et al., 1997; Xiang and Johnston, 1994, 1997; Chlistunoff et al., 1999). To apply this method to the amino acids, we have employed a high-temperature, high-pressure spectrophotometric flow system described in a previous paper by Trevani et al. (2001). The procedure, which is similar in concept to that developed by Chlistunoff et al. (1999), involves preparing buffer solutions of the amino acid, with its sodium and trifluoromethanesulfonate ("triflate") salts, which are pumped through the cell at elevated temperatures. The pH is determined from the spectrum of a trace concentration of the appropriate colorimetric pH indicator which has been added to the buffer solution. The great advantages of this method are its relative ease and its speed. It minimizes the time the amino acid is exposed to elevated temperatures, and thereby extends the temperature range that can be studied without significant decomposition.

Our objective in this work is to apply the hydrothermal pH indicator method to the study of amino acids and peptides in high-temperature water. This paper reports values for the first and second dissociation constants of glycine, and the first dissociation constant of proline and α -alanine at temperatures up to 250°C. Values for the ionization constant of acetic acid were also determined over this range, as a means of testing the validity of these procedures.

2. EXPERIMENTAL

2.1. Materials

α -Alanine was obtained from BDH Ltd. ("Assay 98.5 to 100.5%") and from Aldrich ("Assay 99%"). Before use, the α -alanine was recrystallized according to the method of Perrin and Armarego (1988). L-proline ("Assay 99+%") and glycine ("Assay 99+%") were obtained from Aldrich and used without further purification to prepare stock solutions by mass. Stock solutions of NaOH were prepared from 50% (w/w) (certified) solution of sodium hydroxide obtained from Fisher Scientific. These solutions of NaOH were subsequently standardized by triplicate titration against potassium hydrogen phthalate (Analar, Analytical Reagent) using phenolphthalein as the indicator. The potassium hydrogen phthalate was dried at 105°C to constant mass. Glacial acetic acid was obtained from BDH Ltd. (ACS grade), and diluted stock solutions were standardized by triplicate titration against standard NaOH using phenolphthalein as the indicator. Trifluoromethanesulfonic (triflic) acid, $\text{CF}_3\text{SO}_3\text{H}$, was obtained from Alfa Aesar ("Assay 99%"), and diluted stock solutions were standardized by triplicate pH titration against tris(hydroxymethyl)aminomethane (Aldrich, "Assay 99.9+%") which had been previously dried to constant mass at 105°C. Acridine ("Assay 97%") and 2-naphthol ("Assay 98%") were all obtained from Aldrich and used without further purification. Boiled nanopure water (resistivity $> 16\text{M}\Omega \cdot \text{cm}$) was used for the preparation of all stock and sample solutions.

Buffer solutions of acetic acid were prepared by adding a known mass of aqueous sodium hydroxide to an aliquot of acetic acid solution. Buffer solutions of proline, glycine, and α -alanine were prepared by adding a known mass of either triflic acid or sodium hydroxide to an aliquot of amino acid solution.

For this work, we chose the indicators acridine and 2-naphthol

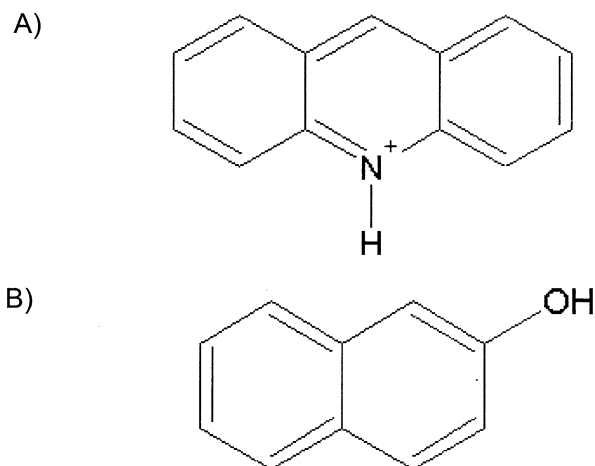


Fig. 1. Colorimetric indicators: (A) acridine and (B) 2-naphthol

because the dissociation constants for these indicators at the temperatures of interest overlap with estimated values of the ionization constants of the amino acids in our study. Acridine was used to determine the carboxylate ionization constants. Values for the ionization constant of the amino group of glycine were determined using 2-naphthol. The molecular structures of these indicators are shown in Figure 1.

The neutral indicators were found to be slow to dissolve in water, so they were either combined with a known mass of dilute triflic acid to form aqueous acridinium triflate or with dilute sodium hydroxide to form the aqueous sodium salt of 2-naphthol, then stirred overnight in sealed Nalgene bottles to ensure complete dissolution. The aqueous indicators are air and light sensitive, so the bottles were wrapped in aluminum foil and contact with air was minimized. Indicator solutions were used immediately after preparation, and a new indicator solution was prepared each night before spectra were to be measured.

The acidic and basic extrema solutions for the indicators were generated as follows. Two aliquots (each ~ 10 mL) of the dissolved acridinium triflate were transferred to 60-mL Nalgene bottles. The solution in the first bottle was diluted to ~ 60 mL with deionized water. This solution formed the acid extremum, containing only the protonated acridinium ion in an excess of triflic acid. ~ 20 mL of 0.3 M NaOH (a twofold excess of base) was added to the second bottle, and the resulting solution was again diluted to ~ 60 mL with deionized water. This solution formed the base extremum, which contained only the neutral acridine species in an excess of sodium hydroxide. For the 2-naphthol solution, this process was reversed. To prepare the basic extremum solutions, an aliquot (~ 10 mL) of the dissolved sodium salt of each indicator was diluted to ~ 60 mL, to yield only the ionic species 2-naphthoxide in an excess of sodium hydroxide. For the acid extremum, a twofold excess of ~ 0.3 M triflic acid was added to an aliquot (~ 10 mL) of dissolved indicator, followed by dilution to ~ 60 mL to yield solutions containing only the neutral species in an excess of triflic acid. At each step of the indicator preparations, the masses of solutions transferred and water added were recorded.

To avoid significant changes to the equilibrium buffer ratio, the indicators had to be added to the buffer systems as neutral solutions. For acridine dissolved in triflic acid, a portion of the original indicator solution was removed and neutralized with sodium hydroxide. For 2-naphthol dissolved in sodium hydroxide, the indicator solution was neutralized with triflic acid. The neutralized indicator solution was added to each buffer solution and the resulting solution was diluted to ~ 60 mL, to achieve a relatively constant indicator concentration and ionic strength in the solutions. Once again the masses of all solution transfers and additions were recorded so that the concentrations and ionic strengths of each solution could be calculated.

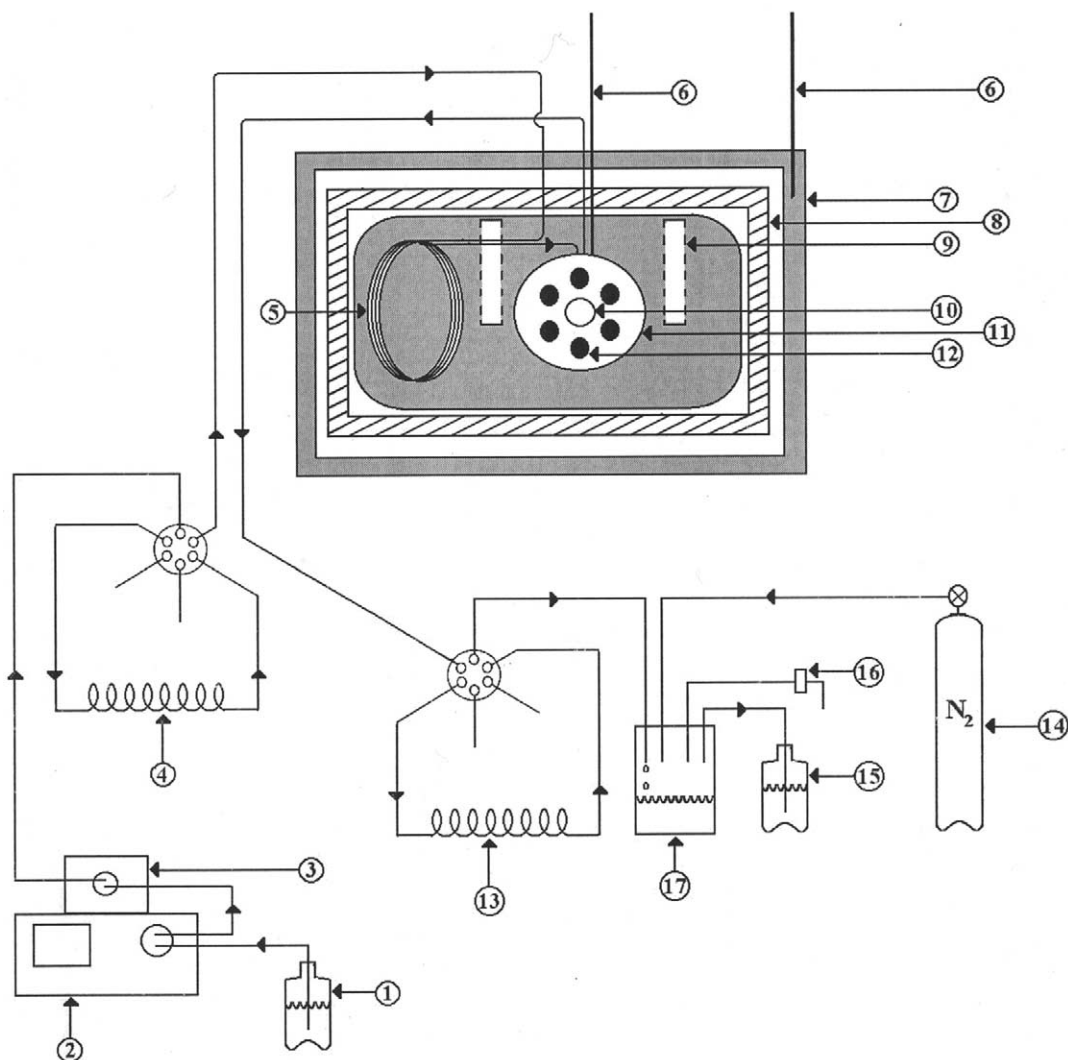


Fig. 2. UV-vis cell and flow injection system: 1, water reservoir; 2, Gilson 305 high-performance liquid chromatography (HPLC) piston pump; 3, Gilson 805 manometric module; 4, injection loop; 5, preheater; 6, Chromega-Alomega thermocouple; 7, brass/aluminum housing; 8, ceramic insulation; 9, cartridge heater; 10, sapphire window; 11, titanium flow cell; 12, bolt; 13, sampling loop; 14, nitrogen cylinder; 15, reservoir for solution effluent; 16, back pressure regulator; 17, stainless steel reservoir.

2.2. Apparatus

A Varian Cary 50 spectrophotometer was used in conjunction with a high-temperature, high-pressure flow system for spectroscopic measurements. The flow system is similar to that developed by Chlistunoff et al. (1999) and was described in a previous paper (Trevani et al., 2001). The cell and injection system are illustrated schematically in Figure 2. Cary Scan Application software was used for data acquisition.

The flow cell was constructed from titanium with a 0.34 cm^3 cylindrical sample chamber bored along the cell's principal axis. Sapphire windows, with Teflon washers as compressible seals, were fixed at each end of the sample compartment by bolted end-plates. The cell was secured in a brass oven and heated using two Chromalux CIR-20203 cartridge heaters. The titanium input tubing was wound around the brass oven to serve as a preheater. The oven was encased in ceramic insulation, then enclosed in an aluminum/brass housing with internal water circulation for cooling. This entire assembly was then placed into the sample chamber of the spectrophotometer. The cell temperature was maintained to $\pm 0.1^\circ\text{C}$ using an Omega CN7600 temperature controller and monitored with a Chromega-Alomega thermocouple located near the sample chamber of the cell.

A Gilson 305 high-performance liquid chromatography (HPLC) piston pump delivered water or the solution at a constant volumetric flow rate. The pressure of the flow system was maintained at 50 ± 5 bar by a nitrogen-filled cylinder and a back-pressure regulator (Tescom model 26-1700). The system pressure was measured by a Gilson 805 manometric module.

2.3. Methods

All spectra were recorded at wavelengths from 250 to 500 nm with a constant volumetric flow rate of $0.2 \text{ cm}^3 \text{ min}^{-1}$. At least two baselines per solution were measured at each temperature to ensure stability. Six spectra of each sample solution were recorded and averaged to minimize noise. Baseline spectra of triflic acid, sodium hydroxide, the acetic acid buffer solutions, and the amino acid buffer solutions were measured at each temperature. None of these solutions had ultraviolet spectra which overlapped those of the indicator solutions, and the baselines for all the buffer solutions except proline were identical with water. At high temperature, the spectrum of aqueous proline was complicated by a broad weak band, shown in Figure 3, that overlaps the

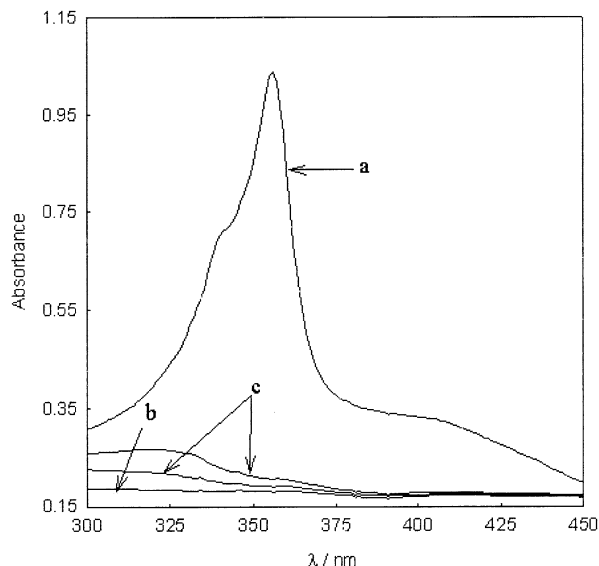


Fig. 3. Comparison of baseline spectra for HPro⁺/Pro[±] buffer solutions at 523.15 K and 45 bar. (a) acridine in proline buffer solution (buffer ratio = 1.2), (b) water without acridine, and (c) proline buffer solutions without acridine (buffer ratios 0.2:1 and 2:1).

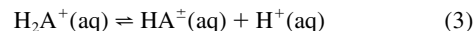
spectrum of acridine. The absorbance of this band increased as the buffer ratio was increased. To overcome this problem, the background spectrum used to correct the measurements on each aqueous proline buffer solution was that of the same proline buffer with no acridine added.

After these measurements were completed, work was reported by other laboratories which indicates that titanium may catalyze the decomposition of amino acids by decarboxylation and other mechanisms (Cox, 2004; Li and Brill, 2003). Our earlier studies in a platinum vibrating tube densitometer and flow microcalorimeter, which used very similar injection systems constructed of platinum (Clarke and Tremaine, 1999; Clarke et al., 2000), showed no detectable decomposition of glycine at 225°C, or of α -alanine and proline at 250°C. We subsequently collected samples of our glycine and proline solutions which had been injected through the titanium UV-visible system at the identical flow rate used in these experiments (0.2 cm³.min⁻¹) for analysis by ¹³C-NMR. NMR spectra were obtained at 150.9 MHz on a Bruker 600 instrument, using the modulated spin echo attached-proton method. These tests did not reveal any decomposition products for glycine at 250°C (detection limit ~1%). However, they did show that proline underwent significant decomposition at 250°C, as indicated by the presence of alkene carbon atoms.

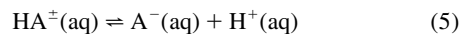
The volume of our system (cell, 0.35 cm³; preheater, 0.30 cm³) is such that solutions injected at a flow rate of 0.2 cm³.min⁻¹ reach the cell in ~2 min, and have a residence time of ~4 min (preheater + cell), before being completely eluted. Calculations using the rate data of Li and Brill (2003) suggest that the degree of decomposition of alanine at 250°C in our system is less than 1%, whereas the degree of decomposition of glycine may be as high as 3% at 225°C and 20% at 250°C. Because the surface to volume ratio in our equipment is lower than that used by Li and Brill, we believe these are upper limits. We know of no published rate constants for proline decomposition; however, the ¹³C-NMR analysis did show significant decomposition products at 250°C and the proline results at this temperature must be taken with caution.

3. SPECTROSCOPIC ANALYSIS

In the analysis that follows, we have used the following equilibria to represent the dissociation of protonated and zwitterionic forms of the amino acids:

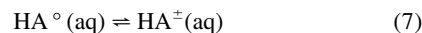


$$K_{a,\text{COOH}} = \frac{m_{\text{H}^+} m_{\text{HA}^\pm} \gamma_{\text{H}^+} \gamma_{\text{HA}^\pm}}{m_{\text{H}_2\text{A}^+} \gamma_{\text{H}_2\text{A}^+}} \quad (4)$$



$$K_{a,\text{NH}_4^+} = \frac{m_{\text{A}^-} m_{\text{H}^+} \gamma_{\text{A}^-} \gamma_{\text{H}^+}}{m_{\text{HA}^\pm} \gamma_{\text{HA}^\pm}} \quad (6)$$

Here, m_{H^+} , m_{HA^\pm} , $m_{\text{H}_2\text{A}^+}$, and m_{A^-} are the molalities of the hydrogen ion and the amino acid in its zwitterionic, protonated and anionic forms, respectively. $K_{a,\text{COOH}}$ and K_{a,NH_4^+} are the thermodynamic equilibrium constants for reactions (3) and (5), respectively. These are determined for the corresponding concentration quotients, $Q_{a,\text{COOH}} = (m_{\text{H}^+} \cdot m_{\text{HA}^\pm})/m_{\text{H}_2\text{A}^+}$ and $Q_{a,\text{NH}_4^+} = (m_{\text{A}^-} \cdot m_{\text{H}^+})/m_{\text{HA}^\pm}$, either by estimating the activity coefficients, γ_i , or extrapolating Q_a to infinite dilution. The equilibrium between zwitterionic and non zwitterionic forms can be represented by:

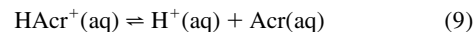


$$K_{\text{HA}^\circ} = \frac{m_{\text{HA}^\pm} \gamma_{\text{HA}^\pm}}{m_{\text{HA}^\circ} \gamma_{\text{HA}^\circ}} \quad (8)$$

We assume K_{HA° is very large so that the concentration of the nonzwitterionic amino acid under these conditions is negligible.

Colorimetric indicators are so called because they exist in two forms, an acid and its conjugate base, which are in equilibrium. Each form has a different UV-visible spectrum. The relative amount of each form depends on the pH so that, when both are present, the spectrum of the mixture is a linear combination of the spectra for the acid and conjugate base. If the spectra of the two forms of the indicator are determined independently, then the ratio of acid to conjugate base in the mixture can be found from its spectrum, and the pH of the solution can be calculated.

This analysis is based on the recently reported values for the temperature-dependent ionization constants for acridine (Ryan et al., 1997) and 2-naphthol (Xiang and Johnston, 1994). The acid dissociation of acridinium ion to acridine can be represented by the expression (Clarke, 2000)



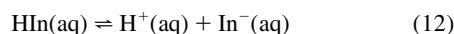
$$K_{\text{HAcr}^+} = \frac{m_{\text{H}^+} m_{\text{Acr}} \gamma_{\text{H}^+} \gamma_{\text{Acr}}}{m_{\text{HAcr}^+} \gamma_{\text{HAcr}^+}} \quad (10)$$

$$\ln K_{\text{HAcr}^+} = -12.43 - 3663.04 \left(\frac{1}{T} - \frac{1}{T_r} \right) - \left(\frac{15874.31}{T} \right) \left(\frac{1}{\epsilon_r} - \frac{1}{78.38011} \right) \quad (11)$$

where T is temperature in Kelvin, $T_r = 298.15$ K, and ϵ_r is the static dielectric constant of water, as reported by Fernandez et al. (1997). The acid dissociation of 2-naphthol can be represented by:

Table 1. Calculated values of $\log K_{\text{HAcr}^+}$ and $\log K_{\text{HIn}}$ used in the calculations.

t (°C)	$\log K_{\text{HAcr}^+}$ (acridine) Eqn. 11	$\log K_{\text{HIn}}$ (2-naphthol) Eqn. 14 and Eqn. 15
25	-5.39	-9.78
50	-5.02	-9.49
75	-4.69	-9.29
100	-4.42	-9.16
125	-4.18	-9.07
150	-3.98	-9.02
175	-3.80	-9.01
200	-3.65	-9.03
225	-3.52	-9.09
250	-3.42	-9.19



$$K_{\text{HIn}} = \frac{m_{\text{H}^+} m_{\text{In}^-} \gamma_{\text{H}^+} \gamma_{\text{In}^-}}{m_{\text{HIn}} \gamma_{\text{HIn}}} \quad (13)$$

where, $\text{HIn}(\text{aq})$ is the neutral, acidic form of the indicator. For 2-naphthol, the acid dissociation constant is given by the expression:

$$\log_{10} K_{2\text{-naphthol}} = -4.186 - \left(\frac{2.822 \cdot 10^3}{T} \right) + \left(\frac{6.245 \cdot 10^5}{T^2} \right) - \left(\frac{8.355 \cdot 10^7}{T^3} \right) + k \cdot \log \rho_w \quad (14)$$

$$k = 7.170 + \left(\frac{3.153 \cdot 10^3}{T} \right) + \left(\frac{9.54 \cdot 10^4}{T^2} \right) \quad (15)$$

where T is temperature in Kelvin and ρ_w is the density of water ($\text{g} \cdot \text{cm}^{-3}$). The values of $\log K$ for acridine and 2-naphthol used in the calculations are reported in Table 1.

The molality of $\text{H}^+(\text{aq})$ can be determined from the indicator ratio through Eqn. 10, $m_{\text{H}^+} = K_{\text{HAcr}^+} (m_{\text{HAcr}^+} / m_{\text{Acr}}) \cdot \{\gamma_{\text{HAcr}^+} / (\gamma_{\text{Acr}} \gamma_{\text{H}^+})\}$. An expression for the first ionization constant for the amino acids is found by substituting the expression for m_{H^+} into Eqn. 4 to yield:

$$K_{\alpha, \text{COOH}} = K_{\text{HAcr}^+} \left(\frac{m_{\text{HAcr}^+}}{m_{\text{Acr}}} \right) \left(\frac{m_{\text{HA}^\pm}}{m_{\text{H}_2\text{A}^+}} \right) \left(\frac{\gamma_{\text{HAcr}^+} \gamma_{\text{HA}^\pm}}{\gamma_{\text{Acr}} \gamma_{\text{H}_2\text{A}^+}} \right) \quad (16)$$

In a directly analogous way, the second dissociation constant is found by rearranging Eqn. 13, to obtain $m_{\text{H}^+} = K_{\text{HIn}} (m_{\text{HIn}} / m_{\text{In}^-}) \cdot \{\gamma_{\text{HIn}} / (\gamma_{\text{In}^-} \gamma_{\text{H}^+})\}$, and substituting into Eqn. 6 to yield:

$$K_{\alpha, \text{NH}_4^+} = K_{\text{HIn}} \left(\frac{m_{\text{A}^-}}{m_{\text{HA}^\pm}} \right) \left(\frac{m_{\text{HIn}}}{m_{\text{In}^-}} \right) \left(\frac{\gamma_{\text{HIn}} \gamma_{\text{A}^-}}{\gamma_{\text{In}^-} \gamma_{\text{HA}^\pm}} \right) \quad (17)$$

The activity coefficients of HA^\pm , acetic acid, and the neutral indicators are assumed to be unity throughout the concentration and temperature ranges. Ionic activity coefficients are assumed to depend solely on charge and ionic strength (Holmes and Mesmer, 1983; Lindsay, 1989, 1990) and thus $(\gamma_{\text{HAcr}^+} / \gamma_{\text{H}_2\text{A}^+}) = 1$ and $(\gamma_{\text{A}^-} / \gamma_{\text{In}^-}) = 1$. With these approximations, Eqns. 16 and 17 are greatly simplified, so that:

$$K_{\alpha, \text{COOH}} = K_{\text{HAcr}^+} \left(\frac{m_{\text{HA}^\pm}}{m_{\text{H}_2\text{A}^+}} \right) \left(\frac{m_{\text{HAcr}^+}}{m_{\text{Acr}}} \right) \quad (18)$$

$$K_{\alpha, \text{NH}_4^+} = K_{\text{HIn}} \left(\frac{m_{\text{A}^-}}{m_{\text{HA}^\pm}} \right) \left(\frac{m_{\text{HIn}}}{m_{\text{In}^-}} \right) \quad (19)$$

The first molality quotient on the right-hand side of each equation is simply the buffer ratio, which can be estimated from the initial composition of the solutions if the contributions for dissociation of the acid or hydrolysis of the conjugate base are negligible. The second ratio, the indicator ratio, is determined from the UV-visible spectrum which is denoted in the discussion below by the wavelength-dependent absorbance $A(\lambda)$. It is important to note that only the indicator *ratio* need to be known, not the individual value of the molality of each indicator species.

It is convenient to designate concentration in units of mol/(kg of solution), m^* , rather than the usual mol/(kg of water), m . In the following derivation, we use HIn^+ to designate the protonated form of the indicator and In^- to designate the deprotonated form; b is the path length; and ρ_{solution} is the solution density. The absorbance of a solution containing the acid and base forms of the indicator is given by Beer's law, using the expression $m^* = C / \rho_{\text{solution}}$ to convert concentrations from molarity, C , to effective molality, m^* :

$$A(\lambda) = [\epsilon_{\text{HIn}^+}(\lambda) b m_{\text{HIn}^+}^* + \epsilon_{\text{In}^-}(\lambda) b m_{\text{In}^-}^*] \rho_{\text{solution}} \quad (20)$$

where $A(\lambda)$ is the absorbance at each wavelength, λ . The terms $\epsilon_{\text{HIn}^+}(\lambda)$ and $\epsilon_{\text{In}^-}(\lambda)$ are the absorptivities of the indicator in the acid form and its conjugate base, as determined from independent experiments with indicator solutions in excess of triflic acid and sodium hydroxide, respectively. These may be expressed as:

$$\epsilon_{\text{HIn}^+}(\lambda) = \frac{A_{\text{acid}}(\lambda)}{b m_{\text{acid}}^* \rho_{\text{acid}}} \quad (21)$$

$$\epsilon_{\text{In}^-}(\lambda) = \frac{A_{\text{base}}(\lambda)}{b m_{\text{base}}^* \rho_{\text{base}}} \quad (22)$$

Substituting these expressions for the absorptivity into Eqn. 20 and rearranging gives

$$\frac{A(\lambda)}{b \rho_{\text{solution}}} = \frac{A_{\text{acid}}(\lambda)}{b m_{\text{acid}}^* \rho_{\text{acid}}} \left(m_{\text{HIn}^+}^* + \frac{\rho_{\text{acid}} A_{\text{base}}(\lambda)}{\rho_{\text{base}} A_{\text{acid}}(\lambda)} D m_{\text{In}^-}^* \right) \quad (23)$$

where $D = m_{\text{acid}}^* / m_{\text{base}}^*$; ρ_{acid} is the density of the acid extremum solution; and ρ_{base} is the density of the base extremum solution. Because the solutions are so dilute, it is reasonable to assume the ratios of the densities will be unity, i.e., $(\rho_{\text{acid}} / \rho_{\text{base}}) \approx 1$, so that

$$A(\lambda) = A_{\text{acid}}(\lambda) \frac{m_{\text{HIn}^+}^*}{m_{\text{acid}}^*} + A_{\text{base}}(\lambda) D \frac{m_{\text{In}^-}^*}{m_{\text{acid}}^*} \quad (24)$$

$$A(\lambda) = A_{\text{acid}}(\lambda) k + A_{\text{base}}(\lambda) D l \quad (25)$$

The constants 'k' and 'l' can be found by least squares regression of the experimental spectra. The indicator ratio is easily found from the expression

$$\frac{k}{l} = \frac{m_{HIn}^*}{m_{In}^*} = \frac{m_{HIn}}{m_{In}} \quad (26)$$

Good agreement between the fitted and the experimental spectra was generally observed, with correlation coefficients better than 0.999. The uncertainty in the fitting parameters depends on the indicator concentration ratio, for most of the solutions the error limits were lower than $\pm 1\%$ with the exception of solutions where one form of the indicator is at very low concentration. These solutions yielded error limits as high as $\pm 4\%$.

Once each indicator ratio was known, the corresponding ionization constants were calculated from Eqns. 18 and 19 using the indicator dissociation constants calculated from either Eqn. 11 or Eqns. 14 and 15, as appropriate. The exact values of the buffer ratios, $m_{HA\pm}/m_{H2A+}$ and $m_{H2A-}/m_{HA\pm}$, were calculated from the initial composition of the solution through charge and mass balance equations.

Decisions on the choice of experimental conditions (i.e., temperature and amino acid buffer ratio) were governed by the need to maintain the buffer ratio in the range 0.1 to 10 (i.e., $0.1 \leq m_{HA\pm}/m_{H2A+} \leq 10$). This is because appreciable molalities of both buffer species are required to maintain a constant, well-defined equilibrium pH. The value of the equilibrium pH is determined by fitting Eqn. 25 to the spectral data. For accurate results, it is desirable to work in a temperature and pH range for which both the acidic and basic forms of the indicator are present in appreciable concentrations.

The method was tested by determining $Q_{a,COOH}$ for acetic acid from 25 to 225°C for comparison with accurate high-temperature potentiometric measurements by Mesmer et al. (1989). The results, which are tabulated in Table A1, reproduced those reported by Mesmer et al. (1989), with a maximum discrepancy of 0.14 $\log K_{a,COOH}$ units and an average discrepancy of $\pm 0.05 \log K_{a,COOH}$. These lie within the combined

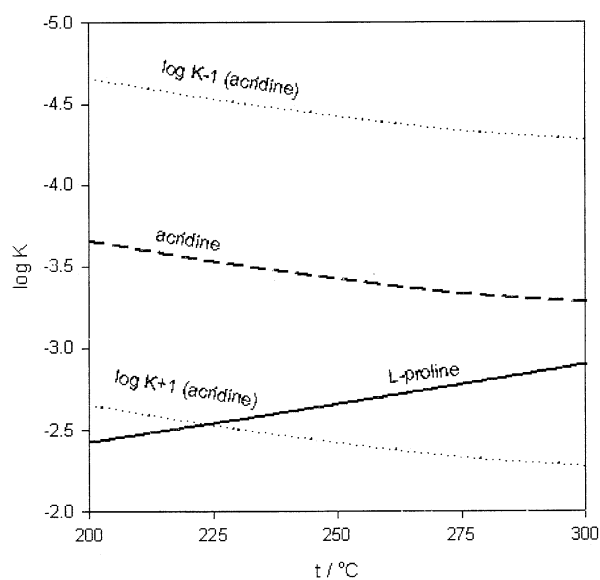


Fig. 4. Predicted indicator range of acridine, defined as $\log K_{HAcr+} \pm 1 \log$ unit, and the temperature dependence of $\log K_{a,COOH}$ of proline, as estimated from room temperature thermodynamic data.

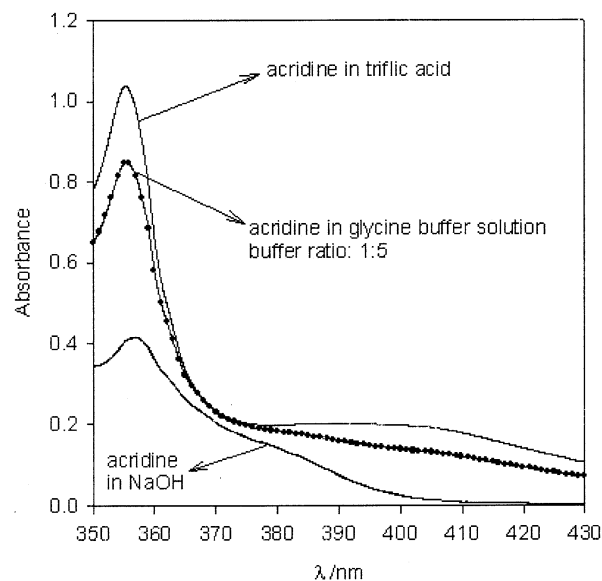


Fig. 5. Comparison of the spectra of acridine at 200°C and 45 bar in triflic acid (acid extremum), sodium hydroxide (base extremum), and glycine buffer solution (1:5 buffer ratio). From top to bottom: —, acridine in triflic acid; —, acridine in glycine buffer solution fitted spectrum, and ●, acridine in glycine buffer solution experimental data; —, acridine in sodium hydroxide.

experimental uncertainties, thus demonstrating that our methodology for measuring the ionization constants of weak acids and bases can yield accurate results.

4. RESULTS

4.1. Carboxylic Acid Ionization Constants for Glycine, α -Alanine, and Proline

The carboxylic acid ionization constants $K_{a,COOH}$ for proline, glycine, and α -alanine were measured by applying the methodology outlined above at temperatures from 150 to 250°C, using acridine as the colorimetric indicator. The temperature range over which both forms of the indicator were present in the buffer solutions was determined by trial and error, guided by the extrapolations of room temperature data. An example is shown in Figure 4, where $\log K_{HAcr+}$ for acridine is plotted along with values for $\log K_{a,COOH}$ for proline extrapolated from room temperature data. The area of overlap between ($\log K_{HAcr+} \pm 1$) and $\log K_{a,COOH}$ corresponds to the expected practical limits of meaningful measurements.

The quality of the spectroscopic data are illustrated by Figure 5, which shows visible spectra of the acridinium ion in aqueous triflic acid (the acid extremum); acridine in aqueous sodium hydroxide (the base extremum); and acridine in a glycine buffer solution with a 1:5 ($m_{HA\pm}/m_{H2A+}$) buffer ratio. As expected, the spectrum of acridine in the buffer solutions is intermediate between the acid and base extrema, reflecting the relative concentration of the two forms of the indicator at each equilibrium pH. Figure 5 shows a comparison of the experimental spectrum with that calculated by linear combination of the extrema spectra, as determined by the regression analysis outlined above. The regression results lead directly to the indicator

Table 2. Experimentally determined values of $\log K_{a,COOH}$ of glycine ($H_3N^+CHCOOH(aq) \rightleftharpoons (H_3N^+)CHCOO^-(aq) + H^+(aq)$).

t (°C)	I (mol kg ⁻¹)	Total glycine (mol kg ⁻¹)	Buffer ratio ^a	Acridine indicator ratio ^b	$\log K_{a,COOH}$	$\log K_{a,COOH}^c$ (avg. values)
150	0.0611	0.1441	12.0	2.89	-2.44	-2.42 ± 0.25
	0.0525	0.0867	5.83	6.52	-2.40	
200	0.0662	0.1346	14.6	0.911	-2.53	-2.61 ± 0.16
	0.0616	0.0775	5.91	2.32	-2.52	
	0.0822	0.0949	2.26	6.43	-2.49	
	0.0852	0.0602	1.22	6.48	-2.76	
225	0.0807	0.0465	0.711	11.4	-2.74	-2.73 ± 0.19
	0.0611	0.1443	11.8	0.477	-2.78	
	0.0524	0.0866	5.66	1.05	-2.76	
250	0.0802	0.0658	1.24	6.16	-2.64	-2.88 ± 0.50
	0.0873	0.0618	1.22	2.90	-2.88	

^a Defined as $m_{HGly\pm}/m_{H_2Gly+}$

^b Defined as $m_{HAcrl\pm}/m_{Acr}$

^c Error limits are 95% confidence intervals for the average values. At 250°C the uncertainty was taken as twice the uncertainty at 150°C.

ratio, $m_{HIn\pm}/m_{In}$, through Eqns. 25 and 26, with relative errors in the individual “k” and “l” coefficients of less than ±2% for each of the four temperatures studied. For acridine the agreement between the fitted and experimental spectra was best within the range 350 and 430 nm, where the differences between the spectra of both forms of the indicator are most pronounced. For 2-naphthol the optimum range is 280 to 370 nm.

Values for the dissociation constants of the carboxylic acid groups of glycine, alanine, and proline, calculated from these results, are listed in Tables 2 to 4 along with the buffer ratio, the indicator ratio, and the ionic strength of each buffer solution. The ionization constants of all three amino acids were found to lie outside the effective range of the acridine pH indicator at temperatures below 150°C.

Carboxylic acid dissociation constants for glycine and proline were obtained from experiments at several different buffer ratios, chosen to optimize the indicator ratios at each temperature. The results had a precision of ± 0.25 $\log K_{a,COOH}$ or better from 150 to 250°C, although we note that the values for proline and, possibly, glycine at 250°C contain an unknown systematic error due to thermal decomposition and must be used with caution. The error limits (precision) were estimated from the 95% confidence limits of the least squares fits and the scatter between results at different buffer ratios.

Buffer ratios near 1.0 were used at all temperatures for alanine, the first system studied, with the result that the indicator ratios at the lowest temperatures are rather high, as is the

estimated uncertainty. The precision, based on 95% confidence limits, improved with increasing temperatures as the indicator ratio moved into the optimum range. The results in Tables 2 to 4 show no statistically significant differences between the values of $K_{a,COOH}$ for all three amino acids over the temperature range covered by this study, despite the fact that proline is a secondary amino acid with a ring structure.

We have estimated the percentage of carboxylic acid in our buffers that would exist as a dimer using the dimerization constants for acetic acid at 25°C reported by Suzuki et al. (1973). The concentration of carboxylic acid in our buffer systems is less than 0.15 mol · kg⁻¹, and dimerization is not significant. Moreover, a Raman study by Semmler and Irish (1988) indicates that lower concentrations of associated species exist in aqueous solutions of acetic acid at elevated temperatures. Thus, any error introduced by neglecting the self-association in our systems is expected to be small and within the experimental uncertainty.

4.2. Ammonium Ionization Constants for Glycine

To measure the ammonium ionization constant for glycine, $K_{a,NH4+}$, 2-naphthol was used as the colorimetric indicator over a temperature range of 75 to 125 °C. The spectra of 2-naphthol in triflic acid (acid extremum); in sodium hydroxide (base extremum); and in Gly⁻/Gly[±] buffer solutions at several different buffer ratios, are shown in Figure 6. A comparison of

Table 3. Experimentally determined values of $\log K_{a,COOH}$ of alanine $CH_3CH(NH_2^+)COOH(aq) \rightleftharpoons CH_3CH(NH_2^+)COO^-(aq) + H^+(aq)$.

t (°C)	I (mol kg ⁻¹)	Total alanine (mol kg ⁻¹)	Buffer ratio ^a	Acridine indicator ratio ^b	$\log K_{a,COOH}^c$
150	0.0489	0.0877	1.04	56.6	-2.22 ± 0.97
175	0.0489	0.0917	1.03	24.7	-2.40 ± 0.41
200	0.0489	0.0939	1.03	12.6	-2.54 ± 0.21
225	0.0489	0.0955	1.03	6.8	-2.68 ± 0.09

^a Defined as $m_{HA1\pm}/m_{H_2A1+}$

^b Defined as $m_{HAcrl\pm}/m_{Acr}$

^c Estimated uncertainties in the $\log K_{a,COOH}$ values are from propagation of the standard deviation of the coefficients “k” and “l” in Eqn. 25.

Table 4. Experimentally determined values of $\log K_{a,COOH}$ of proline ($(C_4H_7)(H_2N^+)COOH(aq) \rightleftharpoons (C_4H_7)(H_2N^+)COO^-(aq) + H^+(aq)$).

t (°C)	I (mol kg ⁻¹)	Total proline (mol kg ⁻¹)	Buffer ratio ^a	Acridine indicator ratio ^b	$\log K_{a,COOH}$	$\log K_{a,COOH}^c$ (avg. values)		
175	0.150	0.8454	8.95	2.87	-2.40	-2.37 ± 0.03		
	0.149	0.7383	7.81	3.52	-2.37			
	0.147	0.6033	6.39	4.48	-2.35			
	0.147	0.5119	5.22	5.29	-2.37			
200	0.159	1.0185	9.92	1.38	-2.52		-2.47 ± 0.04	
	0.151	0.8401	8.79	1.67	-2.49			
	0.151	0.7123	7.69	1.98	-2.48			
	0.148	0.6083	6.25	2.59	-2.45			
	0.147	0.5135	5.12	3.29	-2.43			
225	0.160	1.0163	9.80	0.769	-2.65			-2.69 ± 0.04
	0.151	0.8424	8.66	0.775	-2.7			
	0.150	0.7364	7.55	0.84	-2.73			
	0.148	0.6094	6.15	1.12	-2.69			
250	0.148	0.5124	5.03	1.41	-2.68	-2.73^d		
	0.155	0.3547	2.76	1.73	-2.75			
	0.149	0.2680	2.03	2.86	-2.66			
	0.142	0.1799	1.20	4.31	-2.71			
	0.144	0.1277	0.519	7.75	-2.82			

^a Defined as $m_{HPro^+}/m_{H_2Pro^+}$

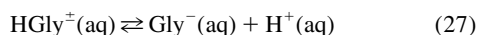
^b Defined as m_{HAcr^+}/m_{Acr}

^c Error limits are 95% confidence intervals for the average values.

^d Evidence of thermal decomposition.

the fitted and experimental spectra for 2-naphthol in the glycine buffer solutions is also included in the figure.

The equilibrium constant $K_{a,NH4^+}$, which corresponds to the ionization of the ammonium group of glycine,



was calculated from the spectral data using Eqns. 17, 25, and 26. The results are summarized in Table 5. Preliminary results

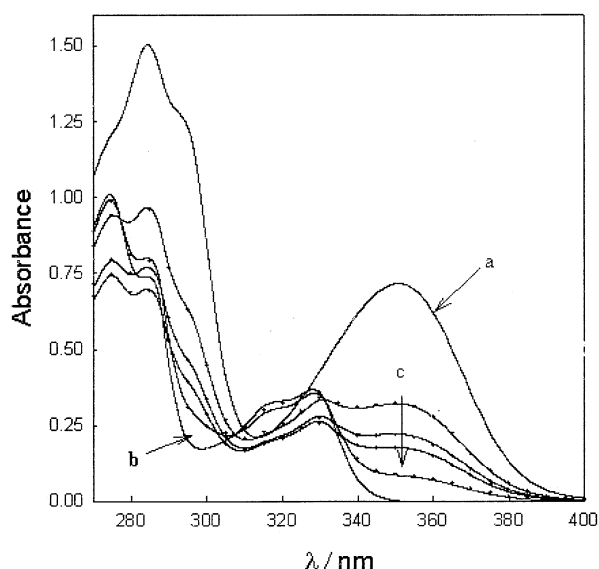


Fig. 6. Comparison of the spectra of 2-naphthol at 125°C and 45 bar in: (a) triflic acid (acid extremum); (b) sodium hydroxide (base extremum); and (c) glycine buffer solutions at Gly^-/Gly^\pm buffer ratios equal to 1, 5, 7, and 10, shown from top to bottom. Symbols are: —, fitted spectrum; ●, experimental data (some points omitted for clarity)

for the second ionization constant of α -alanine using β -naphthoic acid as the colorimetric indicator have also been determined. These are reported in the Ph.D. thesis by Clarke (2000).

5. THERMODYNAMIC MODELS

5.1. Extended van't Hoff Model for Carboxylic Acid Ionization Constants

The experimental $K_{a,COOH}$ data were analyzed using two models. The first was a simple "extended" van't Hoff equation in which the standard partial molar heat capacity of reaction, $\Delta_r C_p^0,COOH$, is independent of temperature:

$$\ln K_{a,COOH}(T) = \ln K_{a,COOH}(T_r) + \frac{\Delta_r H_{a,COOH}^0(T_r)}{R} \left(\frac{1}{T_r} - \frac{1}{T} \right) + \frac{\Delta_r C_p^0,COOH}{R} \left(\ln \left(\frac{T}{T_r} \right) + \frac{T_r}{T} - 1 \right) \quad (28)$$

Here $K_{a,COOH}(T_r)$ and $\Delta_r H_{a,COOH}^0(T_r)$ are the equilibrium constant and enthalpy of reaction at the reference temperature $T_r = 298.15$ K, respectively, and $\Delta_r C_p^0,COOH$ is the mean heat capacity of reaction over the temperature and pressure range of the data used in the fit. To obtain physically meaningful results, the reaction must be carefully chosen to conform with the assumption that $\Delta_r C_p^0,COOH$ is independent of temperature. This can be done by expressing the ionization reaction as an "isocoulombic" (charge-symmetric) equilibrium. Isocoulombic reactions typically have small, almost constant values of $\Delta_r C_p^0,COOH$, resulting in nearly linear plots for $\ln K$ vs. $1/T$ (Mesmer et al., 1988).

Reaction (3) for the first ionization constant of the amino acids is formally "isocoulombic," as it is written, if the zwitterion is regarded as a neutral species. We chose to fit Eqn. 28

Table 5. Experimentally determined values of $\log K_{a,NH4^+}$ for glycine ($H_3N^+CHCOO^-$ (aq) \rightleftharpoons $H_2NCHCOO^-$ (aq) + H^+ (aq)).

t (°C)	I (mol kg ⁻¹)	Total glycine (mol kg ⁻¹)	Buffer ratio ^a	β -Naphthol indicator ratio ^b	$\log K_{a,NH4^+}$	$\log K_{a,NH4^+}$ ^c (avg. values)	
75	0.0112	0.1085	0.104	19.3	-8.99	-8.99 ± 0.08	
	0.0505	0.0985	0.99	2.16	-8.96		
	0.0996	0.1083	9.96	0.246	-9.02		
100	0.0116	0.1076	0.098	47.6	-8.49		-8.54 ± 0.12
	0.0505	0.0980	0.976	4.33	-8.53		
	0.0994	0.1076	7.29	0.502	-8.59		
125	0.0116	0.1076	0.0982	53.7	-8.35	-8.23 ± 0.05	
	0.0219	0.1170	0.208	35.8	-8.2		
	0.0503	0.1469	0.491	14.2	-8.23		
	0.0505	0.0980	0.975	7.13	-8.23		
	0.102	0.1451	2.19	3.59	-8.18		
	0.0994	0.1175	4.54	1.77	-8.17		
0.0996	0.1126	5.88	1.34	-8.17			
0.0994	0.1076	7.10	0.877	-8.28			

^a Defined as $m_{Gly^-}/m_{Gly^{\pm}}$

^b Defined as m_{HIn}/m_{In^-}

^c Errors are 95% confidence intervals for the average values.

to the equilibrium constant data for glycine, alanine, and proline using values of $K_{a,COOH}$ and $\Delta_r H_{a,COOH}^{\circ}$ at 298.15 K fixed to the literature values for glycine and alanine reported by Wang et al. (1996), and to the values for proline compiled by Smith and Martell (1982). The results are tabulated in Table 6, and plotted in Figures 7a and 7b as $\log K_{a,COOH}$ vs. T. Equation 28 was found to fit all amino acids well, with standard deviations for glycine, alanine, and proline of $\sigma_{\log K} = 0.02$, 0.03, and 0.04, respectively. The alanine data at 150°C and 175°C had much larger standard deviations from the spectral fits than those at higher temperatures and those for other amino acids, because the buffer ratios of these (our first) measurements were not varied to optimize the indicator ratios. These are plotted in Figure 7b. As a result, there was considerable uncertainty at these temperatures, and these points were not included in the fit. Although the values of $\Delta_r C_{p,COOH}^{\circ}$ for glycine and alanine would be expected to be very similar, the experimental values are -121 ± 2 and -90 ± 4 J K⁻¹ mol⁻¹, respectively. We believe the total uncertainty of $\Delta_r C_{p,COOH}^{\circ}$ for glycine, including systematic errors, is no more than ± 10 J

K⁻¹ mol⁻¹, whereas that of alanine is larger, perhaps as large as ± 30 J K⁻¹ mol⁻¹. The value for proline, $\Delta_r C_{p,COOH}^{\circ} = -132 \pm 3$ J K⁻¹ mol⁻¹, is more negative with a total uncertainty of the order of ± 10 J K⁻¹ mol⁻¹.

Although the extended van't Hoff model did a good job of reproducing our data to within the experimental uncertainties, the model is of limited value for extrapolating to very high temperatures where C_p° of individual species are known to vary sharply with temperature. An alternative model is presented in the following section.

5.2. "Density" Model for Carboxylic Acid Ionization Constants

Our second approach to modelling the ionization of amino acid carboxylic acid groups made use of the simplified "density" model suggested by Mesmer et al. (1988):

$$\ln K_T = a + \frac{b}{T} + \frac{f}{T} \ln \rho_w \quad (29)$$

Table 6. $\Delta_r C_{p,COOH}^{\circ}$ and $\Delta_r C_{p,NH4^+}^{\circ}$ calculated from extended van't Hoff model.

Amino acid	$\log K_{a,COOH}$ (25°C) ^a	$\Delta_r H_{a,COOH}^{\circ}$ (25°C) (kJ·mol ⁻¹)	$\Delta_r C_{p,COOH}^{\circ}$ (J·K ⁻¹ ·mol ⁻¹)	$\sigma(\log K_{a,COOH})^a$
Glycine	-2.350 ± 0.002^b	4.54 ± 0.41^b	-120.9 ± 2.1^d	0.02
α -alanine	-2.347 ± 0.004^b	2.90 ± 0.37^b	-89.9 ± 3.9^d	0.03
Proline	-1.95^c	1.3 ± 0.1^c	-131.6 ± 3.3^d	0.04
Amino acid	$\log K_{a,NH4^+}$ (25°C)	$\Delta_r H_{a,NH4^+}^{\circ}$ (25°C) (kJ·mol ⁻¹)	$\Delta_r C_{p,NH4^+}^{\circ}$ (J·K ⁻¹ ·mol ⁻¹)	$\sigma(\log K_{a,NH4^+})$
Glycine	-9.78^e	44.4^e	-172.9 ± 41.9	0.13

^a $\log K_{a,COOH} = \ln K_{a,COOH}/2.303$ and $\sigma(\log K_{a,COOH}) = \sigma(\ln K_{a,COOH})/2.303$

^b Average of values reported by Wang et al. (1996).

^c From Smith and Martell (1982).

^d Standard errors from Eqn. 28.

^e From Martell and Smith (1974).

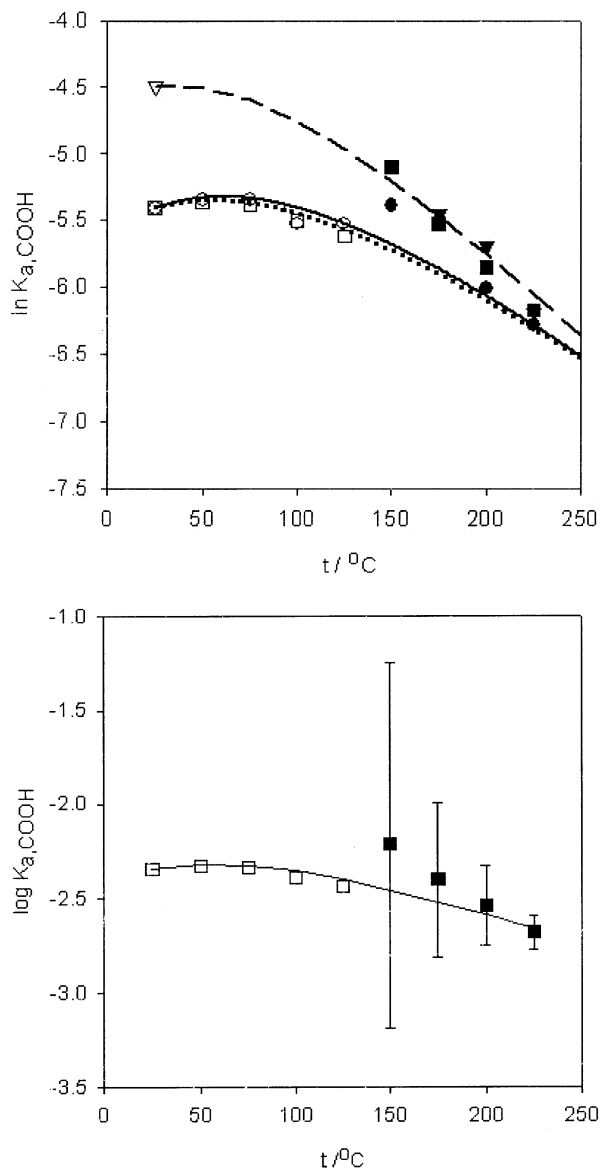


Fig. 7. (a) Extended van't Hoff plot for the first acid dissociation of: \blacktriangledown , - - - - -: proline; \bullet , —: glycine; \blacksquare ,: α -alanine. Open symbols are the corresponding experimental data for glycine and alanine from Wang et al. (1996), and for proline from Smith and Martell (1982). (b) Extended van't Hoff model least squares fit for $\log K_{a,COOH}$, the first acid dissociation of α -alanine showing 95% confidence limits from the fits to indicator spectra: \blacksquare , this work; \square , Wang et al. (1996).

where a , b , and f are adjustable parameters; and ρ_w is the density of water. This model has been used to describe the dissociation of water and many inorganic acids and bases at elevated temperatures and pressures, with much success.

The simplified density model, Eqn. 29 was applied to our data in an attempt to extrapolate $\ln K_{a,COOH}$ to higher temperatures than permitted by the extended van't Hoff model. The parameters 'a' and 'b' can be expressed in terms of $\ln K_{a,COOH}(T_r)$ and $\Delta_r H_{a,COOH}^o(T_r)$ where $T_r = 298.15$ K, so that 'f' becomes the only adjustable parameter (Anderson et al., 1991). This is beneficial here because of the small number of data points.

Equations for $\ln K_{a,COOH}$, $\Delta_r H_{a,COOH}^o$ and $\Delta_r C_{p,COOH}^o$ can be derived from Eqn. 29 using standard thermodynamic relationships :

$$\ln K_{a,COOH}(T) = \ln K_{a,COOH}(T_r) - \frac{\Delta_r H_{a,COOH}^o(T_r)}{R} \left(\frac{1}{T} - \frac{1}{T_r} \right) + \frac{\Delta_r C_{p,COOH}^o}{RT_r(\partial\alpha/\partial T)_{pr}} \left(\frac{1}{T} \ln \frac{\rho_r}{\rho} - \frac{\alpha_r(T - T_r)}{T} \right) \quad (30)$$

$$\Delta_r H_{a,COOH}^o(T) = \Delta_r H_{a,COOH}^o(T_r) + \left(\frac{\Delta_r C_{p,COOH}^o}{Tr(\partial\alpha/\partial T)_{pr}} \right) \left(T\alpha - Tr\alpha_{Tr} + \ln \frac{\rho}{\rho_r} \right) \quad (31)$$

$$\Delta_r C_{p,COOH}^o = \Delta_r C_{p,COOH}^o(T_r) \left(\frac{T(\partial\alpha/\partial T_p)}{Tr(\partial\alpha/\partial T)_{pr}} \right) \quad (32)$$

The density of water ρ , the thermal expansivity $\alpha [= -1/\rho(\partial\rho/\partial T)_p]$, and its slope $(\partial\alpha/\partial T)_p$ were calculated from the NIST database (Harvey et al., 2000).

Equation 30 was fitted to the data in Tables 2 and 3 plus those reported by Wang et al. (1996) for $K_{a,COOH}$ of glycine and α -alanine. The analysis was also applied to data for proline in Table 4, although the lack of data between 25°C and 175°C limited the accuracy of the fit at intermediate temperatures. Values for $K_{a,COOH}(298.15)$ and $\Delta_r H_{a,COOH}^o(298.15)$ for both glycine and α -alanine were fixed to those of Wang et al. (1996), while values from Smith and Martell (1982) were adopted for proline. The calculated parameters 'a', 'b', and the fitted parameter 'f' for Eqn. 29 are given in Table 7. A comparison of the experimental values for $\ln K_{a,COOH}$ and those predicted by the density model is shown in Figure 8. Agreement was very good

Table 7. Density model parameters for Eqn. 29.

Acid	a ^a	b / K ^a	f / K ^b	σ^c
Glycine	-1.909 ± 0.168	-1024.3 ± 49.9	6478.0 ± 104.4	0.05
α -Alanine	-2.981 ± 0.162	-708.4 ± 48.0	4876.0 ± 242.5	0.08
Proline	-2.161 ± 0.075	-674.1 ± 21.6	7019.2 ± 243.0	0.11

^a Estimated uncertainties in the a and b parameters are from propagation of the experimental uncertainties in our "f" fitted parameter value and the reported uncertainties for $\log K_{a,COOH}$ and $\Delta_r H_{a,COOH}^o$ at 25°C.

^b Fitted parameter and standard error from Eqn. 29.

^c Standard deviation of the regression.

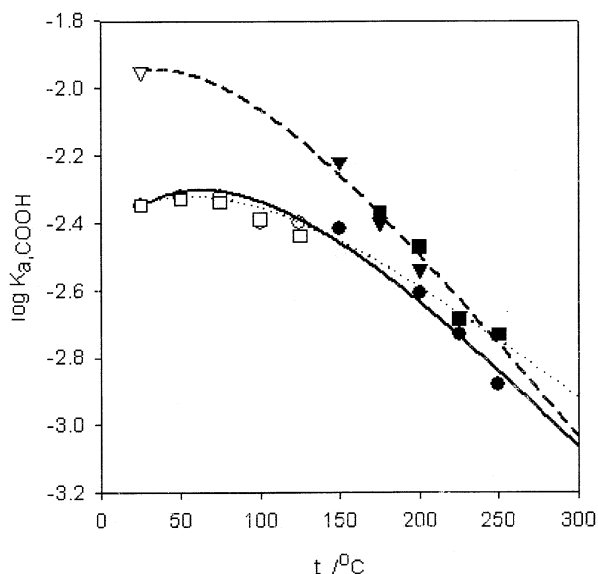


Fig. 8. Density model plot for the first acid dissociation of: ∇ , -----: proline; \bullet , —: glycine; \blacksquare ,: α -alanine. Open symbols are the corresponding experimental data for glycine and alanine from Wang et al. (1996), and for proline from Smith and Martell (1982).

with standard deviations for glycine, alanine, and proline of $\sigma_{\ln K} = 0.05, 0.08,$ and $0.11,$ respectively.

Table 8 summarizes the temperature dependence of $\log K_{a,COOH}, \Delta_r H_{a,COOH}^\circ,$ and $\Delta_r C_{p,COOH}^\circ$ values for glycine, α -alanine, and proline as fitted by the density model. The only adjusted fitting parameter is $\Delta_r C_{p,COOH}^\circ$ at $T = 298.15$ K, which is related to the 'f' parameter (Anderson et al., 1991). The absolute accuracy of our values for $\Delta_r C_{p,COOH}^\circ$ (298 K) of glycine and proline is probably ± 10 J K⁻¹ mol⁻¹, whereas that for alanine is estimated to be ± 30 J K⁻¹ mol⁻¹. The values of $\Delta_r C_{p,COOH}^\circ$ (298 K and 1 bar) = -155 ± 2 J K⁻¹ mol⁻¹ for glycine and $\Delta_r C_{p,COOH}^\circ$ (298 K and 1 bar) = -116 ± 6 J K⁻¹ mol⁻¹ for alanine, compare with the values -137 ± 10 J K⁻¹ mol⁻¹ and -148 ± 10 J K⁻¹ mol⁻¹ reported by Wang et al. (1996), respectively, within the combined precision of all the measurements. The value for proline, $\Delta_r C_{p,COOH}^\circ$ (298 K and 1 bar) = -167 ± 6 J K⁻¹ mol⁻¹ is more negative. This could be due to the thermal decomposition of proline at 250°C, or the difference may be real, reflecting the fact that the proline molecule consists of a ring structure with a secondary amino group, rather than being a simple aliphatic amino acid.

The temperature dependences of $\log K_{a,COOH},$ and $\Delta_r H_{a,COOH}^\circ$ are consistent with those determined by Wang et al. (1996) at

Table 8. Density model predictions for the first dissociation of the amino acids α -alanine, glycine, and proline at 50 bar.^a

t (°C)	$\log K_{a,COOH}$	$\Delta_r H_{a,COOH}^\circ$ (kJ·mol ⁻¹)	$\Delta_r C_{p,COOH}^\circ$ (J·K ⁻¹ ·mol ⁻¹)
Glycine			
25	-2.328 ± 0.002	4.34 ± 0.41	-149.4 ± 2.4
50	-2.291 ± 0.006	1.09 ± 0.41	-115.9 ± 1.9
75	-2.294 ± 0.011	-1.64 ± 0.42	-104.8 ± 1.7
100	-2.324 ± 0.015	-4.24 ± 0.43	-104.9 ± 1.7
125	-2.372 ± 0.018	-6.95 ± 0.45	-113.6 ± 1.8
150	-2.437 ± 0.021	-9.99 ± 0.47	-131.7 ± 2.1
175	-2.518 ± 0.024	-13.65 ± 0.50	-162.7 ± 2.6
200	-2.616 ± 0.027	-18.30 ± 0.55	-214.2 ± 3.5
225	-2.733 ± 0.029	-24.66 ± 0.62	-303.0 ± 4.9
250	-2.878 ± 0.031	-34.09 ± 0.75	-471.1 ± 7.6
Alanine			
25	-2.332 ± 0.004	2.75 ± 0.37	-112.4 ± 5.6
50	-2.311 ± 0.006	0.30 ± 0.39	-87.3 ± 4.3
75	-2.319 ± 0.010	-1.75 ± 0.44	-78.9 ± 3.9
100	-2.347 ± 0.014	-3.71 ± 0.49	-78.9 ± 3.9
125	-2.388 ± 0.017	-5.75 ± 0.57	-85.5 ± 4.3
150	-2.441 ± 0.020	-8.04 ± 0.66	-99.1 ± 4.9
175	-2.505 ± 0.022	-10.79 ± 0.78	-122.5 ± 6.1
200	-2.582 ± 0.024	-14.30 ± 0.93	-161.3 ± 8.0
225	-2.673 ± 0.026	-19.08 ± 1.15	-228.0 ± 11.3
250	-2.785 ± 0.028	-26.18 ± 1.49	-354.6 ± 17.6
Proline			
25	-1.928 ± 0.004	1.08 ± 0.10	-161.9 ± 5.6
50	-1.937 ± 0.004	-2.44 ± 0.16	-125.6 ± 4.4
75	-1.982 ± 0.005	-5.40 ± 0.25	-113.6 ± 3.9
100	-2.051 ± 0.006	-8.22 ± 0.34	-113.6 ± 3.9
125	-2.135 ± 0.006	-1.16 ± 0.44	-123.1 ± 4.3
150	-2.234 ± 0.007	-14.45 ± 0.55	-142.7 ± 4.9
175	-2.346 ± 0.007	-18.41 ± 0.69	-176.3 ± 6.1
200	-2.474 ± 0.008	-23.45 ± 0.86	-232.1 ± 8.0
225	-2.622 ± 0.008	-30.34 ± 1.10	-328.3 ± 11.4
250	-2.797 ± 0.009	-40.56 ± 1.45	-510.4 ± 17.7

^a Calculated values from Eqns. 30, 31, and 32 and coefficients reported in Table 7. Estimated uncertainties in the $\log K_{a,COOH}, \Delta_r H_{a,COOH}^\circ,$ and $\Delta_r C_{p,COOH}^\circ$ values are from propagation of experimental uncertainties in temperature and a, b, and f parameters (Table 7).

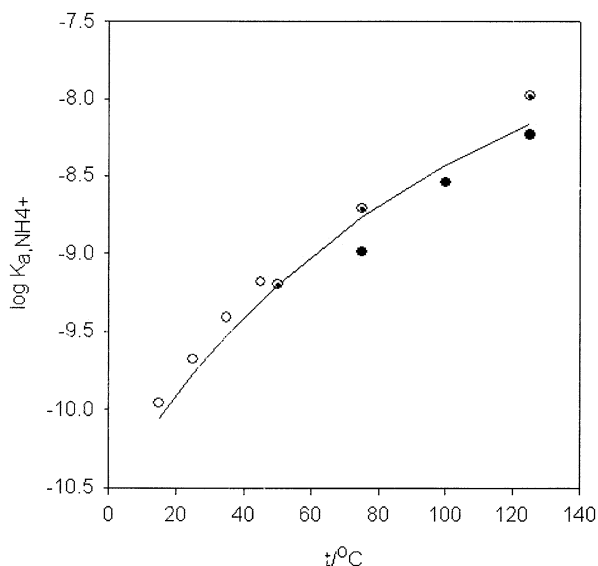


Fig. 9. Extended van't Hoff plot for the second acid dissociation of glycine. ●, experimental; —, calculated values. Experimental data from Smith et al. (1997), ○, and from Gillespie et al. (1995), ⊕, are also shown.

temperatures below 130°C. However, the inclusion of our higher temperature data and the form of Eqns. 29 to 32 causes the slope of $\Delta_r C_{p,COOH}^o$ to be different. Ours is defined by the function $(\partial\alpha/\partial T)_p$ in Eqn. 32, whereas Wang's is based on differentiation of experimental enthalpies of reaction and therefore must be more accurate. Our results extend the temperature range well beyond 125°C, the highest temperature observed by Wang et al. (1996), and show that both $\log K_{a,COOH}$ and $\Delta_r C_{p,COOH}^o$ pass through maxima rather than reaching a plateau. Our reference system, acetic acid, also illustrates this behavior (see Appendix, Table A2).

5.3. Ammonium Ionization Constants

Our experimental values of $\log K_{a,NH4+}$ for glycine are plotted in Figure 9. For glycine $\log K_{a,NH4+}$ values compiled by Smith et al. (1997) and measured values from Gillespie et al. (1995) are included in the plot. Our results are ~3% higher than those of Gillespie et al. (1995) at 75°C and 125°C, which were obtained by titration calorimetry. Both sets of data show a trend towards increasing ionization with increasing temperature with a maximum at some temperature above the range of our measurements.

Due to the limited set of experimental data for glycine, only the extended van't Hoff model was used to analyze the temperature dependence of the second acid dissociation of glycine. Values for $K_{a,NH4+}$ (298.15K) and $\Delta_r H_{a,NH4+}^o$ (298.15K) were fixed to those of Martell and Smith (1974). Both our data and the high-temperature data from Gillespie et al. (1995) were used in the least squares regression. The fitted mean standard partial molar heat capacity of reaction, $\Delta_r C_{p,NH4+}^o = -173 \pm 42 \text{ J.K}^{-1}\text{mol}^{-1}$, is more negative than the value $\Delta_r C_{p,NH4+}^o = -77 \pm 10 \text{ J.K}^{-1}\text{mol}^{-1}$, obtained by Gillespie et al. (1995). Further measurements will be conducted on both glycine,

α -alanine, and proline to extend these results to elevated temperatures.

6. CONCLUSIONS

In this paper we report for the first time values of the first ionization constants for the amino acids proline, glycine, and α -alanine at temperatures greater than 150°C. The first acid dissociation of amino acids is, formally, isocoulombic and should have a reasonably small and constant $\Delta_r C_{p,COOH}^o$. Our data suggest that this is not the case and that, in fact, $\Delta_r C_{p,COOH}^o$ for reaction (3) passes through a maximum then approaches increasingly negative values at elevated temperatures. This is consistent with the fact that the hydrated proton $H^+(aq)$, which is a product in reaction (3), has a smaller effective radius and thus attracts more waters of hydration at elevated temperature than the protonated amino acid, $AH^+(aq)$, which is the reactant (Shock et al., 1992; Mesmer et al., 1988). In addition, although the zwitterionic amino acid product in reaction (3), $AH^+(aq)$, carries no net charge, it also has sufficient polarizing power to increase its hydration under hydrothermal conditions (Clarke and Tremaine, 1999). Finally, these experimental dissociation constants confirm the estimated values used in calculations by Clarke and Tremaine (1999) and Clarke et al. (2000) to show that the standard partial molar volumes and heat capacities of zwitterionic amino acids behave like electrolytes rather than typical non-electrolytes, in that their temperature-dependence is consistent with negative rather than positive discontinuities at the critical point of water.

The excellent agreement with the previous work on acetic acid by Mesmer et al. (1989) confirms findings by Xiang and Johnston (1994, 1997), Ryan et al. (1997), and Chlistunoff et al. (1999) that accurate ionization constants can be obtained with colorimetric indicators under hydrothermal conditions (see also Méndez De Leo et al., 2002). The combination of thermally stable colorimetric indicators with high-pressure flow cells and UV-visible spectrophotometry provides a fast and accurate method for determining dissociation constants for weak acids and bases at extremes of temperature and pressure. The speed afforded by this method makes it very suitable for measuring ionization constants for species with limited hydrothermal stability. Although only a limited number of hydrothermal indicators have been identified and characterized, the temperature range for which each indicator can be used for a given chemical system can be extended by using buffer ratios in the full range from 0.1 to 10. Future work will focus on determining $K_{a,NH4+}$ of glycine, proline, and α -alanine at higher temperatures. This may require finding new indicators for use under more alkaline conditions in hydrothermal solutions (Castet et al., 1991).

Acknowledgments—These measurements were carried out as part of the Ph.D. thesis research by R. Clarke (alanine), and Honours B.Sc. thesis research by C. Collins (glycine) and J. Roberts (proline). We thank the Natural Sciences and Engineering Research Council of Canada (NSERC) for Postgraduate Scholarships to R. Clarke and Summer Undergraduate Scholarships to C. Collins and J. Roberts. Research and equipment grants from NSERC, Memorial University of Newfoundland, and the University of Guelph are gratefully acknowledged. We are also grateful to Mr. Randy Thorne of the Science Machine Shop at

Memorial University for constructing and maintaining the high-temperature flow equipment.

Associate editor: D. Wesolowski

REFERENCES

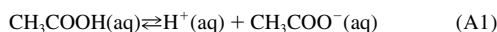
- 1991) The density model for estimation of thermodynamic parameters of reactions at high temperatures and pressures. *Geochim. Cosmochim. Acta* **55**, 1769–1779.
- Bada J. L. and Miller S. L. (1970) The kinetics and mechanism of the reversible nonenzymatic deamination of aspartic acid. *J. Am. Chem. Soc.* **92**, 2774–2782.
- Bada J. L., Miller S. L., and Zhao M. X. (1995) The stability of amino acids at submarine hydrothermal vent temperatures. *Origins of Life and Evolution of the Biosphere* **25**, 111–118.
- Baross J. A. and Deming J. W. (1983) Growth of 'black smoker' bacteria at temperatures of at least 250°C. *Nature* **303**, 423–426.
- Chlistunoff J., Ziegler K. J., Lasdon L., and Johnston K. P. (1999) Nitric / nitrous acid equilibria in supercritical water. *J. Phys. Chem.* **103**, 1678–1688.
- Clarke R. G. and Tremaine P. R. (1999) Amino acids under hydrothermal conditions: Apparent molar volumes of aqueous α -alanine, β -alanine and proline at temperatures from 298 to 523 K and pressures up to 20.0 MPa. *J. Phys. Chem. B* **103**, 5131–5144.
- Clarke R. G., Hnedkovsky L., Tremaine P. R., and Majer V. (2000) Amino acids under hydrothermal conditions: Apparent molar heat capacities of aqueous α -alanine, β -alanine, glycine and proline at temperatures from 298 to 500 K and pressures up to 30.0 MPa. *J. Phys. Chem. B* **104**, 11781–11793.
- Clarke R. G. (2000) Amino acids under hydrothermal conditions: Apparent molar volumes, apparent molar heat capacities, and acid/base dissociation constants for aqueous α -alanine, β -alanine, glycine and proline at temperatures from 25 to 250°C and pressures up to 30.0 MPa. Ph.D. thesis, Memorial University of Newfoundland.
- Cohn E. J. and Edsall J. T. (1943) *Proteins, Amino Acids and Peptides*. Reinhold Publishing Corp., New York, NY, p. 98.
- Cox J. S. (2004) The hydrothermal stability of selected amino acids, Dissertation fur Doktorin der Naturwissenschaften, ETH, Zurich.
- Crabtree R. H. (1997) Where smokers rule. *Science* **276**, 22219.
- Fernandez D. P., Goodwin A. R. H., Lemmon E. W., Levelt Senger J. M. H., and Williams R. C. (1997) A formulation of the static permittivity of water and steam at temperatures 238 to 873 K at pressures up to 1200 MPa, including derivatives and Debye-Hückel coefficients. *J. Phys. Chem. Ref. Data* **26**, 1125–1169.
- Gillespie S. E., Oscarson J. L., Izatt R. M., Wang P., Renuncio J. A. R., and Pando C. (1995) Thermodynamic quantities for the protonation of amino acid amino groups for 325.15 to 398.15 K. *J. Solution Chem.* **24**, 1219–1247.
- Hakin A. W., Duke M. M., Groft L. L., Marty J. L., and Rushfeldt M. L. (1995) Calorimetric investigations of aqueous amino acid and dipeptide systems from 288.15 to 328.15 K. *Can. J. Chem.* **73**, 725–734.
- Hakin A. W., Daisley D. C., Delgado L., Liu J. L., Marriott R. A., Marty J. L., and Tompkins G. (1998) Volumetric properties of glycine in water at elevated temperatures and pressures measured with a new optically driven vibrating tube densimeter. *J. Chem. Thermodynam.* **30**, 583–606.
- Harvey A. H., Peskin A. P., and Klein S. A. (2000) *NIST/ASME Steam Properties Version 2.2*. National Institute of Standards and Technology (U. S. Department of Commerce), Gaithersburg, MD.
- Ho P. C., Bianchi H., Palmer D. A., and Wood R. H. (2000) A new flow-through cell for precise conductance measurements of aqueous solutions to high temperatures and pressures. *J. Solution Chem.* **29**, 217–235.
- Holmes H. F. and Mesmer R. E. (1983) Thermodynamic properties of aqueous solutions of the alkali metal chlorides to 250°C. *J. Phys. Chem.* **87**, 1242–1255.
- Izatt R. M., Oscarson J. L., Gillespie S. E., Grimsrud H., Renuncio J. A. R., and Pando C. (1992) Effect of temperature and pressure on the protonation of glycine. *Biophys. J.* **61**, 1394–1401.
- Li J. and Brill T. B. (2003) Spectroscopy of hydrothermal reactions, Part 26: Kinetics of decarboxylation of aliphatic amino acids and comparison with rates of racemization. *Int. J. Chem. Kinetics* **35**, 602–610.
- Lindsay W. T. Jr. (1989) Computer modelling of aqueous systems in power cycles. In *Properties of Water and Steam* (eds. M. Pichal and O. Sifner), pp. 29–38. Hemisphere Publishing, New York, NY.
- Lindsay W. T. Jr. (1990) Chemistry of steam cycle solutions: Principles. In *The ASME Handbook on Water Technology for Thermal Power Systems* (ed. P. Cohen), Chap. 7, pp. 341–544. Amer. Soc. Mech. Eng., New York, NY.
- Lvov S. N., Zhou X. Y., and Macdonald D. D. (1999) Flow-through electrochemical cell for accurate pH measurements at temperatures up to 400°C. *J. Electroanal. Chem.* **463**, 146–156.
- Martell A. E. and Smith R. M. (1974) *Critical Stability Constants. Volume 1: Amino Acids*. Plenum Press, New York.
- Méndez De Leo L. P., Bianchi H. L., and Fernández-Prini R. J. (2002) Thermodynamics of 4-methylphenol dissociation in water at high temperature using UV-vis spectroscopy. *J. Chem. Thermodynam.* **34**, 1467–1479.
- Mesmer R. E., Baes C. F. Jr., and Sweeton F. H. (1970) Acidity measurements at elevated temperatures. IV. Apparent dissociation product of water in 1M potassium chloride up to 292°C. *J. Solution Chem.* **74**, 1937–1942.
- Mesmer R. E., Marshall W. L., Palmer D. A., Simonson J. M., and Holmes H. F. (1988) Thermodynamics of aqueous association and ionization reactions at high temperatures and pressures. *J. Solution Chem.* **17**, 699–718.
- Mesmer R. E., Patterson C. S., Busey R. H., and Holmes H. F. (1989) Ionization of acetic acid in NaCl(aq.) media: A potentiometric study to 573 K and 130 bar. *J. Phys. Chem.* **93**, 7483–7490.
- Mesmer R. E., Palmer D. A., Simonson J. M., Holmes H. F., Ho P. C., Wesolowski D. J., and Gruszkiewicz M. S. (1997) Experimental studies in high temperature aqueous chemistry at Oak Ridge National Laboratory. *Pure Appl. Chem.* **69**, 905–914.
- Miller S. L. and Bada J. L. (1988) Submarine hot springs and the origin of life. *Nature* **334**, 609–611.
- Patterson C. S., Slocum G., Busey R. H., and Mesmer R. E. (1982) Carbonate equilibrium in hydrothermal systems: First ionization of carbonic acid in NaCl media to 300°C. *Geochim. Cosmochim. Acta* **44**, 1653–1663.
- Perrin D. D. and Armarego W. L. F. (1988) *Purification of Laboratory Chemicals*, 3rd ed Permagon Press, New York.
- Povoledo D. and Vallentyne J. R. (1964) Thermal reaction kinetics of the glutamic acid-pyruvoglutaric acid system in water. *Geochim. Cosmochim. Acta* **28**, 731–734.
- Ryan E. T., Xiang T., Johnston K. P., and Fox M. A. (1997) Absorption and fluorescence studies of acridine in subcritical and supercritical water. *J. Phys. Chem. A* **101**, 1827–1835.
- Semmler J. and Irish D. E. (1988) Vibrational spectral studies of solutions at elevated temperatures and pressures IX: Acetic acid. *J. Solution Chem.* **17**, 805–824.
- Shock E. L. (1990) Do amino acids equilibrate in hydrothermal fluids? *Geochim. Cosmochim. Acta* **54**, 1185–1189.
- Shock E. L. (1992) Stability of peptides in high temperature aqueous solutions. *Geochim. Cosmochim. Acta* **56**, 3481–3491.
- Shock E. L., Oelkers E. H., Johnson J. W., Sverjensky D. A., and Helgeson H. C. (1992). Calculation of the thermodynamic properties of aqueous species at high pressures and temperatures. *J. Chem. Soc. Faraday Trans.* **88**, 803–826.
- Smith R. M. and Martell A. E. (1982) *Critical Stability Constants. Volume 5: First Supplement*. Plenum Press, New York.
- Smith R. M., Martell A. E., and Motekaitis R. J. (1997) *NIST Critically Selected Stability Constants of Metal Complexes Database Version 4.0*, National Institute of Standards and Technology (U. S. Department of Commerce), Gaithersburg, MD.
- Suzuki K., Taniguchi Y., and Watanabe T. (1973) The effect of pressure on the dimerization of carboxylic acids in aqueous solution. *J. Phys. Chem.* **77**, 1918–1922.
- Sweeton F. H., Mesmer R. E., and Baes C. F. Jr. (1973) A high temperature flowing emf cell. *J. Phys. E, Sci. Instr.* **6**, 165–168.

- Trent J. D., Chastain R. A., and Yayanos A. A. (1984) Possible artefactual basis for apparent bacterial growth at 250°C. *Nature* **307**, 737–740.
- Trevani L. N., Roberts J. C., and Tremaine P. R. (2001) Copper(II)-ammonia complexation equilibria in aqueous solutions at temperatures from 30 to 250°C by visible spectroscopy. *J. Solution Chem.* **30**, 585–622.
- Vallentyne J. R. (1964) Biogeochemistry of organic matter - II. Thermal reaction kinetics and transformation products of amino compounds. *Geochim. Cosmochim. Acta* **28**, 157–188.
- Vallentyne J. R. (1968) Pyrolysis of proline, leucine, arginine and lysine in aqueous solution. *Geochim. Cosmochim. Acta* **32**, 1353–1356.
- Wang P., Oscarson J. L., Gillespie S. E., Izatt R. M., and Cao H. (1996) Thermodynamics of protonation of amino acid carboxylate groups from 50 to 125 °C. *J. Solution Chem.* **25**, 243–265.
- Xiang T. and Johnston K. P. (1994) Acid-base behavior of organic compounds in supercritical water. *J. Phys. Chem.* **98**, 7915–7922.
- Xiang T. and Johnston K. P. (1997) Acid-base behavior in supercritical water: β -naphthoic acid–ammonia equilibrium. *J. Solution Chem.* **26**, 13–30.
- Yanagawa H. and Kojima K. (1985) Thermophilic microspheres of peptide-like polymers and silicates formed at 250°C. *J. Biochem.* **97**, 1521–1524.

APPENDIX

Equilibrium Quotient, Q_a , for Acetic Acid

To validate our methodology, we used the hydrothermal colorimetric indicator acridine to measure the concentration quotient for the acid dissociation of acetic acid for comparison with accurate potentiometric data reported by Mesmer et al. (1989). This dissociation can be written as:



with

$$Q_{a,\text{COOH}} = m_{\text{H}^+} \frac{m_{\text{CH}_3\text{COO}^-}}{m_{\text{CH}_3\text{COOH}}} \quad (\text{A2})$$

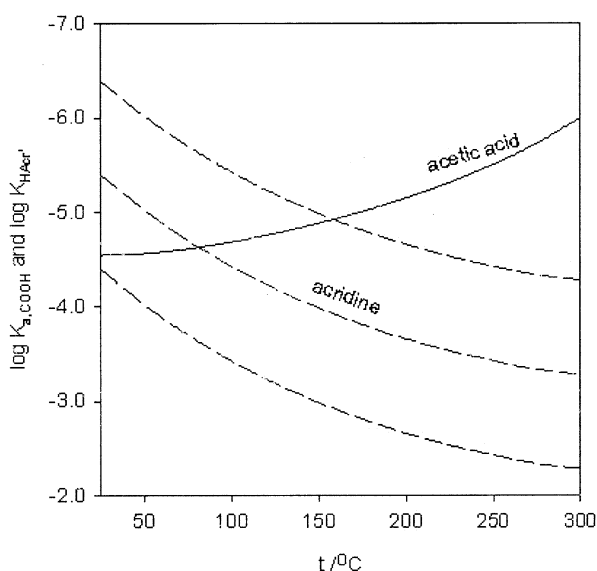


Fig. A1. Comparison of $\log K_{a,\text{COOH}}$ for acetic acid with the predicted indicator range of acridine: —, $\log K_{a,\text{COOH}}$ of acetic acid (Mesmer et al., 1989); —, $\log K_{\text{HAcr}^+} \pm 1$ log unit.

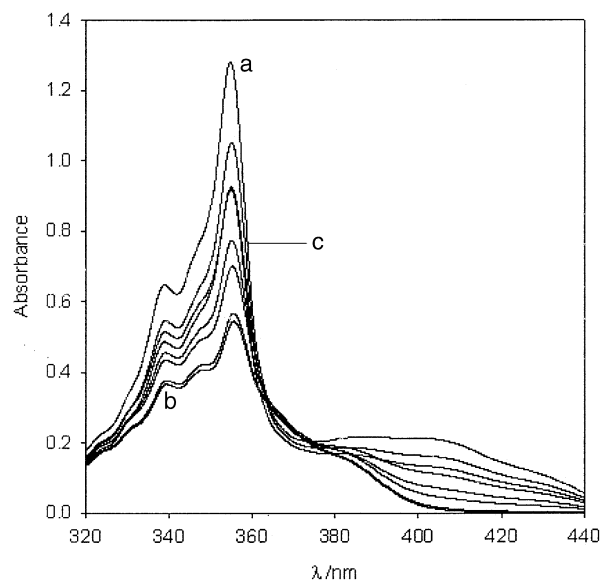


Fig. A2. Spectra of acridine at 175°C and 45 bar: (a) acridine in 0.0387 mol kg^{-1} triflic acid (acid extremum) (b) acridine in acetate/acetic acid buffer solutions, ratios: 5:1, 2:1, 1:1, 0.5:1, 0.2:1, and 0.1:1; (c) acridine in 0.0455 mol kg^{-1} sodium hydroxide (base extremum).

where $Q_{a,\text{COOH}}$ is the molality quotient for reaction A1. Equation 10 can be rearranged to obtain $m_{\text{H}^+} = K_{\text{HIn}}(m_{\text{HIn}}m_{\text{In}})^{-1}\gamma_{\text{HIn}}/(\gamma_{\text{In}}\gamma_{\text{H}^+})$ and substituted into Eqn. A2 to give:

$$Q_{a,\text{COOH}} = K_{\text{HAcr}^+} \frac{\gamma_{\text{HAcr}^+}\gamma_{\text{Acr}}m_{\text{HAcr}^+}m_{\text{CH}_3\text{COO}^-}}{\gamma_{\text{H}^+}m_{\text{Acr}}m_{\text{CH}_3\text{COOH}}} \quad (\text{A3})$$

As before, $\gamma_{\text{HAcr}^+}/\gamma_{\text{H}^+}$ is approximated as 1 and γ_{Acr} is assumed to be 1, giving:

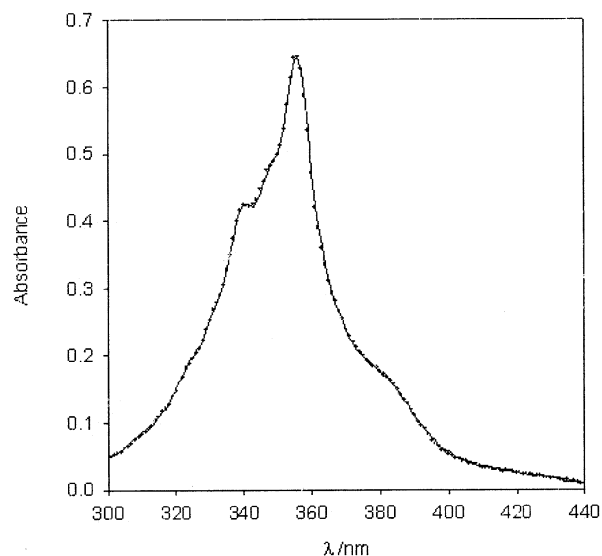


Fig. A3. Experimental and fitted spectra of acridine in (0.0826 mol kg^{-1} sodium acetate + 0.1084 mol kg^{-1} acetic acid) buffer solution at 175°C and 45 bar: ●, experimental points, some omitted; —, least squares regression to Eqn. 25.

Table A1. Comparison of literature and experimental values of log Q_a for acetic acid.

t (°C)	I (mol kg ⁻¹)	Buffer ratio	Indicator ratio	log Q_a (exp.)	log Q_a (lit.) ^a
25	0.132	15.0	0.516	-4.51	-4.52
	0.145	3.24	2.43	-4.5	-4.51
	0.133	1.07	6.02	-4.59	-4.52
50	0.147	10.8	0.298	-4.51	-4.53
	0.150	3.47	0.935	-4.5	-4.52
	0.153	1.43	2.22	-4.51	-4.52
75	0.130	0.638	4.74	-4.53	-4.53
	0.142	7.71	0.198	-4.51	-4.57
	0.146	3.32	0.465	-4.5	-4.57
	0.146	1.24	1.22	-4.51	-4.57
	0.141	0.631	2.33	-4.53	-4.57
100	0.142	0.225	5.99	-4.56	-4.57
	0.144	3.15	0.194	-4.63	-4.64
	0.150	1.47	0.413	-4.64	-4.64
	0.146	0.626	0.943	-4.65	-4.64
	0.129	0.235	2.31	-4.68	-4.65
	0.150	0.123	3.76	-4.52	-4.63
125	0.150	3.69	0.0714	-4.76	-4.72
	0.148	1.43	0.183	-4.76	-4.72
	0.144	0.591	0.426	-4.78	-4.73
	0.155	0.246	0.98	-4.8	-4.72
	0.159	0.133	1.70	-4.83	-4.72
150	0.153	1.27	0.0943	-4.9	-4.82
	0.163	0.715	0.160	-4.92	-4.82
175	0.154	0.661	0.117	-4.91	-4.94
	0.155	0.233	0.284	-4.98	-4.94
	0.164	0.120	0.518	-5.01	-4.93
200	0.163	0.262	0.113	-5.18	-5.07
	0.163	0.119	0.230	-5.21	-5.07
225	0.148	0.115	0.156	-5.26	-5.24

^a Calculated from Model II of Mesmer et al. (1989).

$$Q_{a,COOH} = K_{HAcr^+} \frac{m_{HAcr^+} m_{CH_3COO^-}}{m_{Acr} m_{CH_3COOH}} \quad (A4)$$

The temperature dependences of log $K_{a,COOH}$ and log K_{HAcr^+} are plotted in Figure A1. The region where log $K_{a,COOH}$ lies within ± 1 log unit of log K_{HAcr^+} , $t \leq 150^\circ\text{C}$, is the practical working range of an equi-molar acetate/acetic acid buffer solution. This working range was extended up to $t \leq 225^\circ\text{C}$ by using lower buffer ratios.

Figure A2 shows visible spectra at 175°C of the acridinium ion (acridine in triflic acid; the acid extremum), acridine (acridine in sodium hydroxide; the base extremum), and acridine in acetate/acetic acid buffer solutions ratios (5:1, 2:1, 1:1, 0.5:1, 0.2:1, and 0.1:1). The spectrum of the acridine in the buffer is intermediate between the acid and base extrema, and is a linear combination of the two extreme

spectra ratioed to account for their difference in concentration. Figure A3 plots a comparison of the linear combination of the extrema spectra and the experimental data. Agreement between the calculated and the experimental spectra lies within 1% over the wavelength range 300–450 nm, with the exception of solutions having a very low relative concentration of the acidic or basic forms of the indicator for which the discrepancies can be as high as 4%.

The least squares regression results led directly to the indicator ratio, through Eqns. 25 and 26. The values of K_{HAcr^+} were calculated from Eqn. 11 and summarized in Table 1. From these results the concentration quotient ($Q_{a,COOH}$) of acetic acid was calculated from Eqn. A4. The results are summarized in Table A1. The $Q_{a,COOH}$ values calculated from Mesmer et al. (1989) are included for comparison.

Table A2. Density model predictions for the dissociation of acetic acid.

t (°C)	log $K_{a,COOH}$ ^a	$\Delta_r H_{a,COOH}^\circ$ ^a (kJ mol ⁻¹)	$\Delta_r C_p^{COOH}$ ^a (J K ⁻¹ mol ⁻¹)
25	-4.79 \pm 0.09 (-4.76) ^b	-0.346 (-0.506) ^b	-214 (-144) ^b
100	-5.01 \pm 0.09 (-4.94) ^b	-12.6 (-11.0) ^b	-150 (-154) ^b
200	-5.60 \pm 0.11 (-5.52) ^b	-32.7 (-32.5) ^b	-311 (-300) ^b
300	-6.61 \pm 0.17 (-6.44) ^b	-109.4 (-80.1) ^b	-2280 (-1150) ^b

^a Calculated values according to Eqns. 30, 31, and 32.

^b Mesmer et al. (1989).